Clim Dyn (2015) 44:1901–1918
DOI 10.1007/s00382-014-2272-8

Assessing the effect of domain size over the Caribbean region using the PRECIS regional climate model

Abel Centella-Artola · Michael A. Taylor · Arnoldo Bezanilla-Morlot · Daniel Martinez-Castro · Jayaka D. Campbell · Tannecia S. Stephenson · Alejandro Vichot

Received: 29 November 2013 / Accepted: 21 July 2014 / Published online: 29 July 2014

Abstract This study investigates the sensitivity of the one-way nested PRECIS regional climate model (RCM) to domain size for the Caribbean region. Simulated regional rainfall patterns from experiments using three domains with horizontal resolution of 50 km are compared with ERA reanalysis and observed datasets to determine if there is an optimal RCM configuration with respect to domain size and the ability to reproduce important observed climate features in the Caribbean. Results are presented for the early wet season (May–July) and late wet season (August–October). There is a relative insensitivity to domain size for simulating some important features of the regional circulation and key rainfall characteristics e.g. the Caribbean low level jet and the mid summer drought (MSD). The downscaled precipitation has a systematically negative precipitation bias, even when the domain was extended to the African coast to better represent circulation associated with easterly waves and tropical cyclones. The implications for optimizing modelling efforts within resource-limited regions like the Caribbean are discussed especially in the context of the region's participation in global initiatives such as CORDEX.

Keywords RCM evaluation · Domain size assessment · Caribbean-Central America · Regional climate · CORDEX

A. Centella-Artola (✉) · A. Bezanilla-Morlot · D. Martinez-Castro · A. Vichot
Instituto de Meteorologia, Havana, Cuba
e-mail: abel.centella@insmet.cu

M. A. Taylor · J. D. Campbell · T. S. Stephenson
Department of Physics, University of the West Indies, Mona, Kingston, Jamaica

1 Introduction

Regional climate models (RCMs) have been developed 'as a magnifying glass tool' to increase the resolution of climate projections in specific regions of the globe. Global climate model (GCM) outputs are considered coarse for regional climate change impacts assessments (IPCC 2007). The higher resolution of RCMs enable more detailed representation of local processes, coastlines, land use and topography, which may contribute to the simulation of meaningful small-scale features over limited regions at affordable costs compared to GCMs (Jones et al. 1995; Denis et al. 2002). Higher resolution may also better capture storms and extreme weather (Huntingford et al. 2003; Seneviratne et al. 2012).

One-way nested RCMs integrate atmospheric model equations on a high resolution domain using global model or analysis data as boundary conditions (Christensen et al. 1997; Seth and Giorgi 1998). Several issues arise in setting up RCM nesting experiments including the choice of resolution and the definition of the domain (Giorgi and Mearns 1999). Studies indicate the importance and impact of domain size and the position of the lateral boundaries on simulated regional climate variability (e.g. Jones et al. 1995, 1997; Jacob and Podzun 1997; Colin et al. 2010). Domain size has received more attention as the nesting issue is more a boundary value problem than an initial value problem (Denis et al. 2002). Giorgi and Mearns (1999) note that it is difficult to define general criteria for choosing the domain size as it will depend on the region and experiment design. For example, while Jones et al. (1995) finds a stronger dependence of the United Kingdom Meteorological Office Unified Regional Climate model's results on domain size over Europe, Bhaskaran et al. (1996) shows that the same RCM applied over the Indian monsoon

region does not exhibit similar sensitivity. The Caribbean comprises islands of varying small sizes making it suitable for study using RCMs. The Caribbean is surrounded by the Atlantic Ocean, the Caribbean Sea and the Gulf of Mexico, and is limited by the coasts of North and South America. Granger (1985) characterizes Caribbean climate as diverse, with as many climate types as islands. Tropical and extra-tropical systems interact (Alfonso and Naranjo 1996) and frequently produce complex meteorological conditions. More than 70 % of the rainfall occurs from May to October (November in the eastern Caribbean) due to events embedded in the synoptic easterly flow (e.g. easterly waves and tropical cyclones). Rain is also associated with moisture surges from the Pacific and the Caribbean Sea that impinge upon island topography (Hastenrath 1967) and sea-breeze circulation in islands and peninsulas (Riehl 1979).

The bimodality of the annual rainfall regime is a significant feature of Caribbean climate i.e. the rainy season is characterized by two maxima occurring in May–June and September–October separated by a relatively drier period (July–August) often called the mid-summer Drought (MSD) (Magaña et al. 1999). Tropical cyclone activity in the Caribbean follows a similar bimodal pattern (Inoue et al. 2002). The MSD is associated with the seasonal intensification of the North Atlantic subtropical high (NASH) and low-level regional circulation features such as the Caribbean Low-Level Jet (CLLJ) (Wang 2007; Wang and Lee 2007; Whyte et al. 2008). The strengthening of the low-level easterlies results in stronger vertical wind shear which reduces convective activity over the region (Wang and Lee 2007). The predominantly ocean areas also play an important role in modulating climate variability via the influence of sea surface temperatures (Taylor et al. 2002, 2011; Stephenson et al. 2007; Karmalkar et al. 2012).

Most of the previous sensitivity studies of RCMs to domain size have dealt with continental or semi-continental regions dominated by land areas (Jones et al. 1995; Bhaskaran et al. 1996; Seth and Giorgi 1998). RCM studies for domains including the Caribbean have primarily focused on simulated seasonal precipitation and temperature regimes (Martinez-Castro et al. 2006; Karmalkar et al. 2008, 2012; Tourigny and Jones 2009; Campbell et al. 2010; Diro et al. 2012; Taylor et al. 2013). To the best of our knowledge only Martinez-Castro et al. (2006) have conducted an RCM sensitivity study of Caribbean climate to domain size, resolution and convective schemes using RegCM3 and simulating the 1993 summer period. They find substantial sensitivity to all 3 factors.

In the last few years, the PRECIS RCM (Jones et al. 2004) has been extensively evaluated over the Caribbean and used to produce future regional climates (Centella et al. 2008; Campbell et al. 2010; Karmalkar et al. 2012; Taylor et al. 2013). The RCM studies were developed under the PRECIS-Caribbean project (Taylor et al. 2013) as a part of the coordinated work of the Caribbean Climate Modelling Group (CCMG) comprising institutions from Cuba, Jamaica, Belize, Barbados and Suriname and supported by the Caribbean Community Climate Change Centre. For these studies the choice of domain size and resolution was guided by general criteria i.e. that the domains represented areas large enough to allow the development of regional scale circulations but not so large to prevent the RCM deviating from the GCM in the center of the domain (Campbell et al. 2010). This study explores the impact of the choice of domain size on the downscaled climate since running larger domains is computationally expensive (e.g. longer run time, larger storage requirements) and often results in the need for compromises (e.g. restricting the resolution) where resources for modelling are limited. This study examines the feasibility of an optimal PRECIS domain configuration with respect to domain size, computational resources, and the ability to reproduce important climatic features in the Caribbean. The skill of the PRECIS RCM and the 'added value' of utilizing it in simulating the climate over the Caribbean region are also investigated.

The remainder of the paper is structured as follows. Section 2 describes the PRECIS RCM, the experiments performed and the observational data used for the assessment. Results depicting and comparing model simulations of interannual and intraseasonal variations in rainfall with emphasis on spatial patterns and annual cycles are presented in Sect. 3. Results for model simulations of the MSD and the low-level circulation related with the CLLJ are also presented and examined in the same section. A summary and discussion of the results are provided in Sect. 4.

2 Model, data and methods

2.1 Model description

The study uses the Hadley Centre's regional climate modeling system—PRECIS. It is a hydrostatic primitive equations grid point model containing 19 levels in a vertical hybrid coordinate system (Simmons and Burridge 1981). The horizontal resolutions are 0.44° × 0.44° and 0.22° × 0.22° which gives a minimum resolution of ~50 and ~25 km, respectively at the equator of the rotated grid. Due to its fine resolution, the model requires a timestep of 5 and 2.5 min, respectively to maintain numerical stability. The RCM uses a relaxation technique implemented across a four point buffer zone at each vertical level. The atmospheric sulphur cycle, dynamical flow, radiative processes, clouds and precipitation, the land surface and the deep soil are described in the model. Jones et al. (2004) gives a full description of the model's physics.

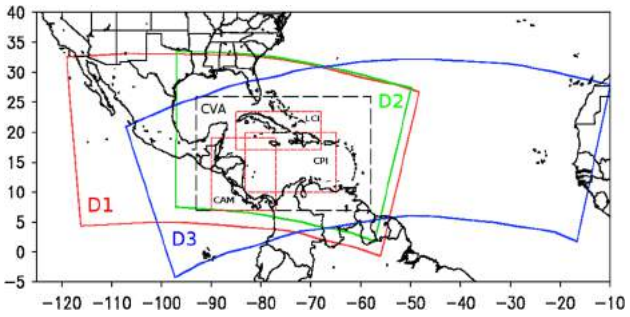

Fig. 1 Domains (excluding the eight point boundary buffer zone) of configurations D1 (*red line*), D2 (*green line*) and D3 (*blue line*) of the regional climate model. The Common Validation Area (CVA) is delimited by *long dash blank line*. *Red boxes* delimit the subregions for which the annual cycle is analyzed-Central America (CAM), Caribbean Precipitation Index (CPI; see the text for definition) and Large Caribbean Islands (LCI)

For this study, initial and lateral boundary forcing is taken from the six hourly fields of a quasi-observed dataset derived from the ERA-interim reanalysis (ERA) at a resolution of 1.5° × 1.5° (Simmons et al. 2007; Dee et al. 2011). The sea surface temperatures (SSTs) and sea-ice fractions surface boundary conditions are taken from a combination of the monthly HadISST1 (Rayner et al. 2003) and weekly NCEP (Kalnay et al. 1996; Kanamitsu et al. 2002) observed datasets. Observed values of various greenhouse gases are used to provide relevant information on atmospheric composition.

2.2 Experiments

PRECIS RCM simulations were made for the years 1990–1999 for three different domains at a resolution of 0.44° × 0.44°. To allow for model spin-up the first year is not considered.

Figure 1 shows the three domain areas after an 8-point buffer zone has been removed. The first domain (D1) mirrors that used in previous PRECIS studies of the Caribbean (e.g. Centella et al. 2008; Campbell et al. 2010; Taylor et al. 2013). The second domain (D2) is smaller and centered over the Caribbean region. Its selection was based mainly on its relatively low computational cost i.e. if results for this smaller domain are comparable to those from larger domains, then its use in future modelling studies will reduce the expense, both in processing time and storage capacity, of producing ensembles of Caribbean climates. This is important given the current institutional capacity within the Caribbean. The third domain (D3) is larger, with the eastern boundary shifted to explicitly include the circulation associated with easterly waves and tropical cyclones as they leave west Africa. These systems have a decisive influence on the accumulated rainfall over areas within the Caribbean.

The default model configuration does not include many of the smaller islands of the eastern Caribbean. A significant additional difference between D3 and the other two domains is the inclusion of the eastern Caribbean islands in D1 and D2 by a filling of the nearest or covering grid boxes as land. (The RCM has the ability to define new land points.) In D3, however, the filling is not done and the eastern Caribbean is defined as sea. The effect of including or excluding the island chain is also explored in the following sections.

A common validation area (CVA) is used for the analysis and comparison of the three domains (Fig. 1). The CVA was located far from the outer domain borders in order to avoid spurious influences of the lateral boundary conditions (LBCs). Within the CVA three other areas are defined—Central America (CAM), the Caribbean Precipitation Index (CPI) region, and the Largest Caribbean Islands (LCI). CAM is a continental region where the signal of the MSD is clearly observed and where the direct influence of the Pacific Ocean is present. The CPI region is as defined by Chen and Taylor (2002) and is often taken as representative of the region's rainfall variability. It is also where the CLLJ occurs. LCI incorporates the larger island territories within the Caribbean. The rainfall climatology of the LCI is also bimodal but the two peaks occur in different months from those of the CAM region.

Analysis was conducted for the wet season in the Caribbean (May–October) and specifically for months representing the early wet season (EWS) (May–July) and the late wet season (LWS) (August-October) (Chen and Taylor 2002). The main focus is on precipitation because of its relevance in most regional climate impact studies, its importance to the hydrological cycle, and its use as an indicator of the freshwater availability of the Caribbean region.

Apart from the domains chosen, the CORDEX protocol was generally followed particularly in terms of the resolution employed and the use of lateral boundary conditions from reanalysis of observations.

2.3 Observational datasets

To assess the model's ability to capture the seasonal precipitation patterns several observational datasets are used as comparison. These include the observed land-only gridded datasets of the Climate Research Unit TS 3.1 (CRU) (Mitchell and Jones 2005), the University of Delaware (UDEL) (Matsuura and Willmott 2007) and the Global Precipitation Climatology Centre (the VASclimO dataset) (Beck et al. 2005). These global datasets have a spatial resolution of 0.5° × 0.5° and are based on station

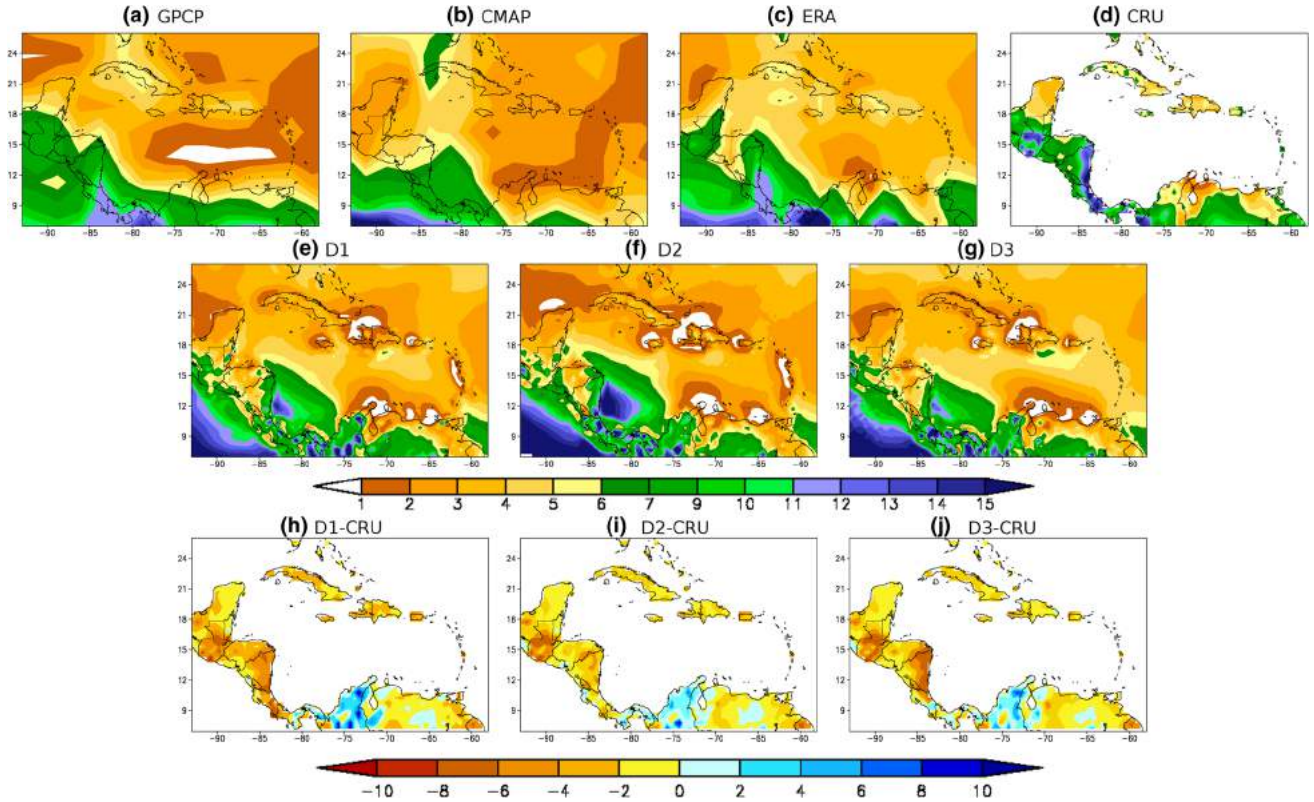

Fig. 2 EWS rainfall climatologies for 1991–1999 in mm/day for **a**–**d** reference fields GPCP, CMAP, ERA and CRU, **e**–**g** simulated values for D1–3 and **h**–**j** anomalies of the simulations with respect to CRU observed climatologies

observations. They differ in the included set of station observations and in the interpolation methods used.

Because of the dominant ocean influence in determining the background climatology of the region, the skill of the RCM in reproducing the large-scale pattern is also assessed through comparison to lower spatial resolution gridded datasets over land and sea. These include the Global Precipitation Climatology Project (GPCP) 2.5° × 2.5° monthly (Adler et al. 2003) and daily (GPCP_1DD) 1° × 1° datasets (Huffman et al. 2001), and the Climate Prediction Center (CPC) Merged Analysis Precipitation (CMAP) dataset (Xie and Arkins 1997). These gridded datasets merge gauge measurements, satellite estimates and model output of rainfall. Use is also made of the International Satellite Cloud Climatology Project (ISCCP) monthly total cloud cover dataset at a resolution of 2.5° × 2.5° (Rossow and Schiffer 1991).

A third group of reference datasets include the ECMWF ERA-interim reanalysis and the National Center for Environmental Prediction (NCEP) North American Regional Reanalysis (NARR) (Mesinger et al. 2006). NARR is a long-term, high-resolution atmospheric and land surface hydrology dataset for the North American domain. Variables extracted from both datasets include evaporation, cloud cover, and those related to atmospheric circulation (e.g. sea level pressure, geopotential height, wind components). Rainfall is not extracted from NARR because analysis (not shown) revealed extremely low values over Caribbean land areas, and unrealistic wet season totals. Since the ERA-Interim data is also the LBC for the regional model, the comparison of the ERA dataset with the model output gives an indication of the 'added value' of downscaling over the driving dataset.

3 Results

3.1 Multiannual spatial patterns

PRECIS shows reasonable skill in reproducing the synoptic scale climatological patterns of precipitation across the Caribbean basin irrespective of domain configuration. Figures 2 and 3 show the EWS and LWS rainfall patterns, respectively for GPCP, CMAP, ERA, CRU and D1–3 over the CVA. In both seasons, notwithstanding domain choice, the precipitation maximum off the Caribbean coastline of Panama associated with the CLLJ (Whyte et al. 2008) is captured, though the model simulates more rain than in

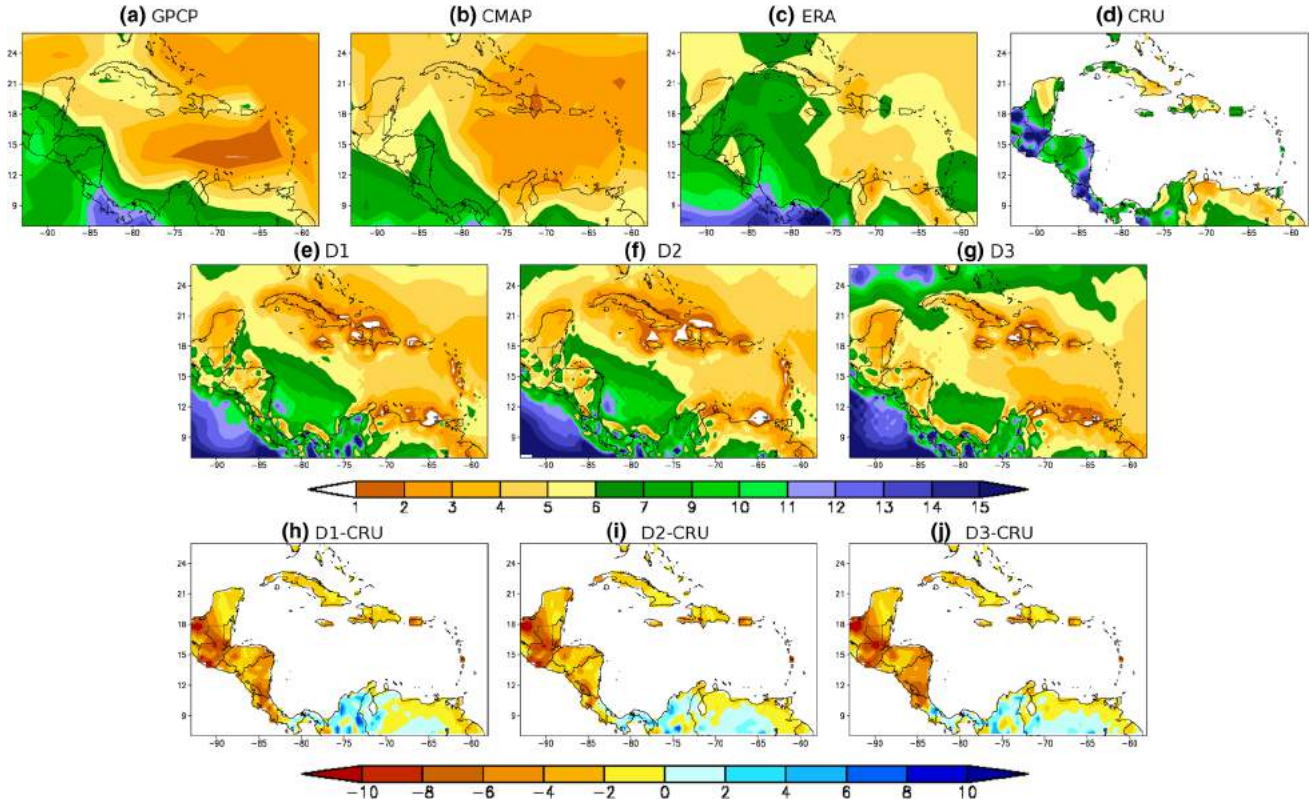

Fig. 3 As Fig. 2, but for LWS

the observed datasets and extends the zone further to the east (Figs. 2e–g, 3e–g). Similarly, the rainfall maximum in the equatorial Pacific close to Panama is well-simulated but anomalously extended to the north-west, appearing as an overestimation of the precipitation associated with the Inter Tropical Convergence Zone (both in intensity and extension). Other captured large-scale features include the dry belt over the southern Dutch Caribbean Islands and the zonal bands of low/high precipitation over central/west Nicaragua. The simulated spatial features of Figs. 2 and 3 mirror the results of Campbell et al. (2010).

Much of the rainfall in the region is convective in origin. The model captures this but underestimates rainfall over most of the CVA. With respect to the ERA dataset (not shown) rainfall is underestimated for all domain experiments and for both seasons, suggesting differences in the simulated large-scale precipitation, particularly over land areas. Comparisons to the CRU dataset (Figs. 2h–j, 3h–j) show the underestimation of rainfall by the model over most land areas. The underestimation is largest (in excess of 2–6 mm/day) over Guatemala and the Caribbean coast of Honduras and Nicaragua, and more intense for D1 and D3. The negative bias is also evident over the Caribbean Islands but it is less intense. Wet biases are confined to Panama and over sections of Colombia and Venezuela.

For both the EWS (Fig. 4) and LWS (not shown) the modeled moisture fluxes from the surface into the atmospheric boundary layer are consistently 10–20 % lower over most land areas than for the ERA reanalysis for all domain simulations. This suggests that the hydrological cycle is less active over land areas in the model. This is discussed further in ensuing sections. In Fig. 4b, c a meridional band of negative values is also observed over the eastern Caribbean which is not present in D3 (Fig. 4d). The presence of land points in D1 and D2 modifies the spatial pattern of the moisture fluxes anomalies.

The three RCM domain experiments reproduce similar large-scale cloud anomaly patterns with respect to ERA for the EWS (Fig. 5) and LWS (not shown). In general, PRECIS simulates less cloud cover over coastal South America, but there are differences between D2 and the other two experiments over Central America and the larger Caribbean Islands. In D2 the cloud anomalies are positive, which likely accounts for smaller negative rainfall anomalies observed over these regions in the D2 simulation (see again Figs. 2, 3). There is also a discernible difference in simulated cloud cover over the eastern Caribbean due to the absence of land points in D3. The simulated cloud patterns are similar to those derived from ISCCP cloud cover data (not shown).

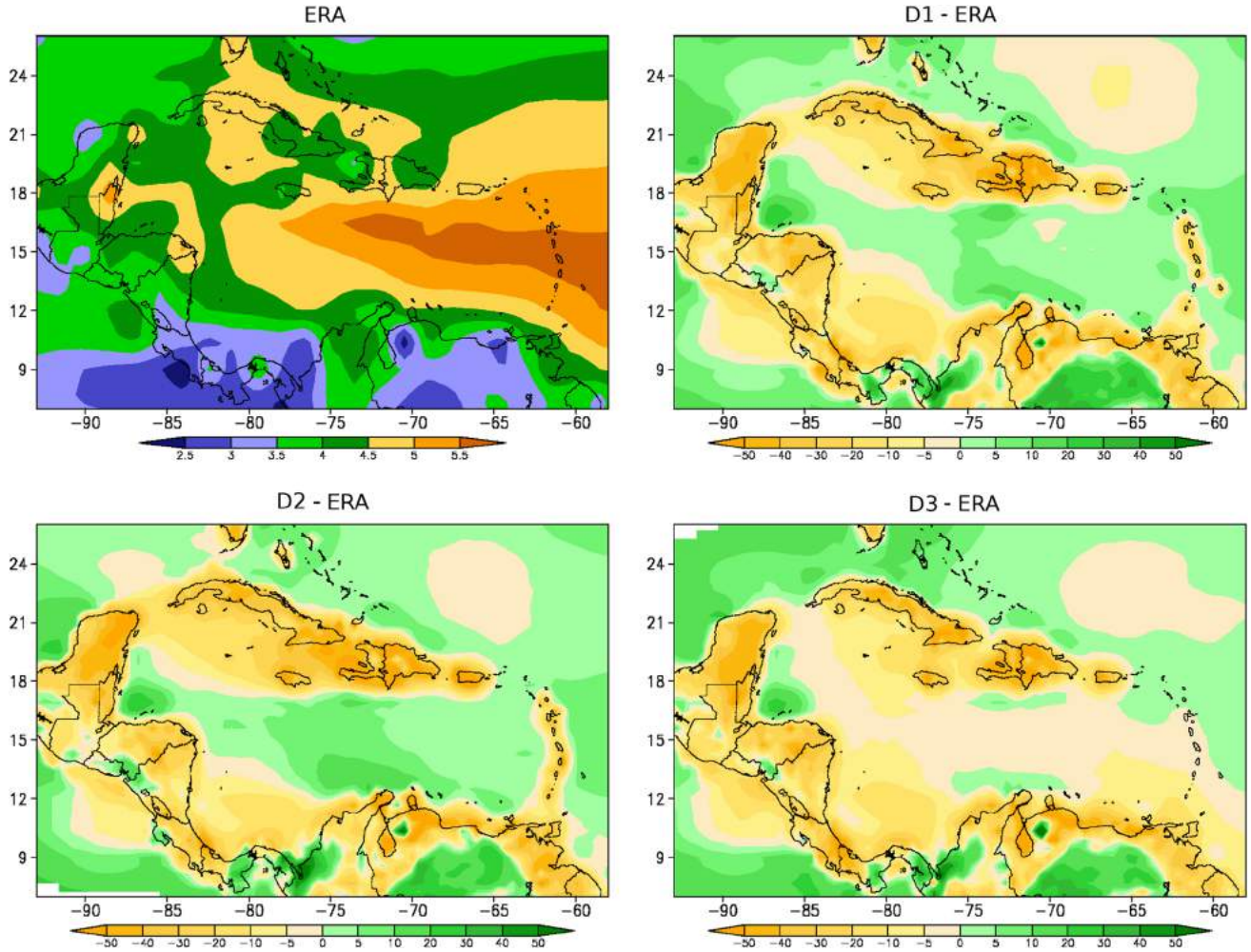

Fig. 4 EWS mean evaporation in mm/day 1991–1999 for ERA; and evaporation differences for D1 minus ERA, D2 minus ERA and D3 minus ERA in percent

Figure 6 explores the impact of changing the model domain on the distribution of daily rainfall over the region. Changes in boundary locations trigger internal variability in the RCM which likely impact day-to-day variability more so than the mean climatology. Results are presented for the frequency and intensity of wet days (hereafter FWD and IWD, respectively) which are defined as rainfall amounts greater than 0.1 mm. The results are presented as differences with respect to the GPCP daily precipitation dataset. For the EWS, the large-scale anomaly patterns of FWD and IWD are similar across all simulations except over the eastern Caribbean in D3. In general, the model produces largest differences in FWD over the sea (Fig. 6, top row). FWD is underestimated over almost all the land areas with anomalies generally greater than 10 %, except over parts of Central and South America. The model simulates higher IWD values (Fig. 6, bottom row) over the Pacific and the southwestern Caribbean Sea i.e. over the same areas where seasonal total precipitation is also higher (see again Fig. 2e–g). In other regions of the CVA IWD anomalies are negative and larger over sea than over land.

Similar results are attained if the simulated FWD and IWD are compared with values derived from the ERA-Interim daily precipitation dataset (not shown). In this case the three model configurations yield fewer wet days over ocean areas and smaller reductions in rainfall intensity.

In an attempt to further delineate differences in the performance of the three RCM configurations in reproducing the seasonal patterns of rainfall and the other related variables, Taylor Diagrams (Taylor 2001) are presented. The Taylor diagrams combine pertinent metrics—in this case the root mean square (RMS) difference, the pattern of correlation (PC) and the standard deviation (STD)—to quantify the similarities or differences between the RCM simulations and a reference field. By normalizing both the simulated RMS and STD with the standard deviation of the

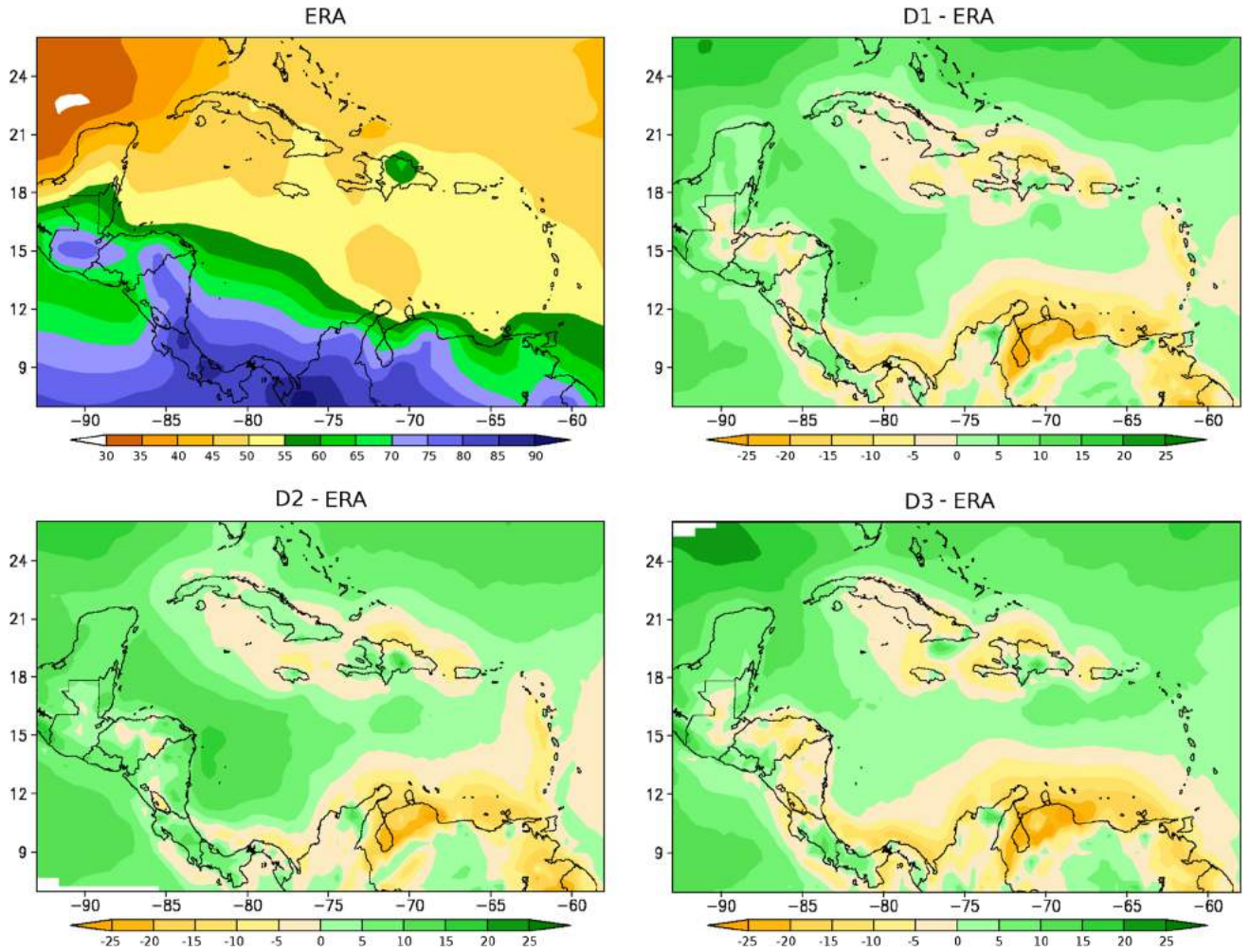

Fig. 5 EWS mean cloud cover (in percent) 1991–1999 for ERA; and cloud cover differences for D1 minus ERA, D2 minus ERA and D3 minus ERA (in percent)

corresponding reference fields, it is possible to combine different fields on the same graph, allowing for a concise summary of the model skill. On the diagrams the reference point (called REF) is plotted at unit distance from the origin along the x-axis, and the distance between REF and individual points correspond to RMS difference. The nearer a simulation result is to REF is the better its performance.

For the EWS, Fig. 7 shows the Taylor Diagrams for precipitation (top row) and for evaporation, cloud cover, FWD and IWD (bottom row), over land-sea grid points (left panels) and land-only grid points (right panels). The results for the LWS yield similar conclusions and are not shown. For precipitation a fourth reference dataset is included in each case (i.e. for the land + sea and land-only diagrams) by averaging the three original datasets used as reference in each case (i.e. ERA, GPCP and CMAP for the land + sea plot and CRU, UDEL and VASClimO for the land only plot). Although the reference datasets are not truly independent, this is done to highlight the spread amongst the reference data (black dots in top row). Figure 7 shows that, though for precipitation the reference datasets are correctly phased in space (i.e. with similar patterns of correlation), they possess some obvious differences in spatial amplitudes (i.e. STD).

With respect to precipitation over land and sea regions the different domain configurations are similarly correlated with observations (depending on the reference dataset) with the main difference being largest amplitudes in D2, though D1 and D3 also show higher amplitudes than observed. Over land areas the differences between domain configurations are mainly associated with the magnitudes of spatial correlation and not so much with amplitudes. For land only points D2 appears to be marginally more skillful as it has greater spatial correlation and smaller RMS difference than D1 and D3. It is clear that the RCM always overestimates the STD and its skill is better over land + sea areas,

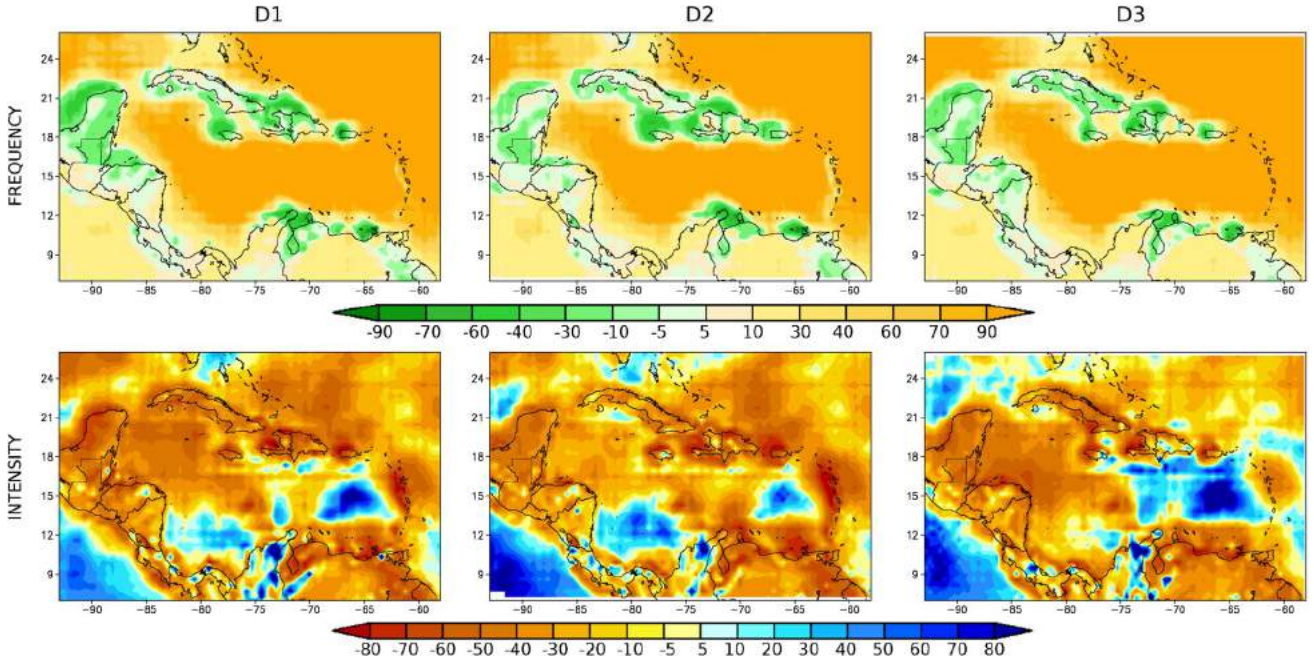

Fig. 6 1991–1999 EWS differences in mean number of rainy days (*top row*) and mean intensity of rainfall (*bottom row*) events between D1–3 and ERA reanalysis. Units expressed as percentage of ERA reanalysis values

as evidenced by higher correlations than for land-only grid points.

Cloud cover is well-reproduced over both the land and land + sea grid points irrespective of domain (green points in bottom row figures). The RCM configurations also do a better job of simulating IWD (with generally similar skill for all configurations) than FWD. Though the differences are not considerable, D2 appears to be the worst at capturing FWD over land + sea points but in contrast has marginally better skill over land points. Evaporation is very poorly represented over land areas irrespective of domain, with very low patterns of correlation and high RMS difference. It is, however, more realistic over sea areas contributing to improved results for land + sea grid points. This reinforces the idea that modeled soil moisture content may be an important cause for the weaker hydrological cycle over land.

In general, for precipitation and for the other related-variables analyzed, the similarities between D1 and D3 (save for those differences due to the absence of Eastern Caribbean land points) suggest no significant alteration of model skill when the right domain border is shifted further to the east. More visible impacts, but in our opinion not so important, are produced when the domain size is reduced on the western side (as in D2), which likely impacts aspects of the circulation associated with Atlantic-Pacific gradients. This bears further investigation.

Finally, an interesting aspect of the modeled rainfall patterns is the presence of dry areas in the form of a precipitation shadow leeward of most of the islands (see again Figs. 2e–f, 3e–f). The feature is not present in the GPCP and CMAP datasets, perhaps due to their lower spatial resolution. Similar dry shadow areas can, however, be found in the TRMM 3B43 highest resolution dataset (Huffman et al. 2007) for the period of 1998–1999, over the southern Caribbean Netherland Antilles and around La Hispaniola and the Yucatan Peninsula (not shown). The driest band over and leeward of the Eastern Caribbean Islands also appears but it is neither as intense nor so close to the islands. This phenomenon in the simulations might be associated with the high sensitivity of the RCM to the land surface and topography configuration i.e. changes in land and vegetation can change the moisture and latent heat fluxes locally, in turn affecting the subregional atmospheric circulation, cloud cover and precipitation over these areas. It is noted that although the precipitation shadow appears in all three domains, it does not occur in D3 for the Eastern Caribbean islands. The same effect can be seen in Campbell et al. (2010) (see the middle row of Fig. 2 in that paper) though the authors do not make reference to it.

3.2 Annual cycle and mid-summer drought

The main feature of precipitation over the Caribbean is a well-defined annual cycle, which exhibits maximum precipitation from May to November and a dry period peaking in February–March. The wet season is bimodal (Chen et al. 1997) with peaks in May–June (early season) and

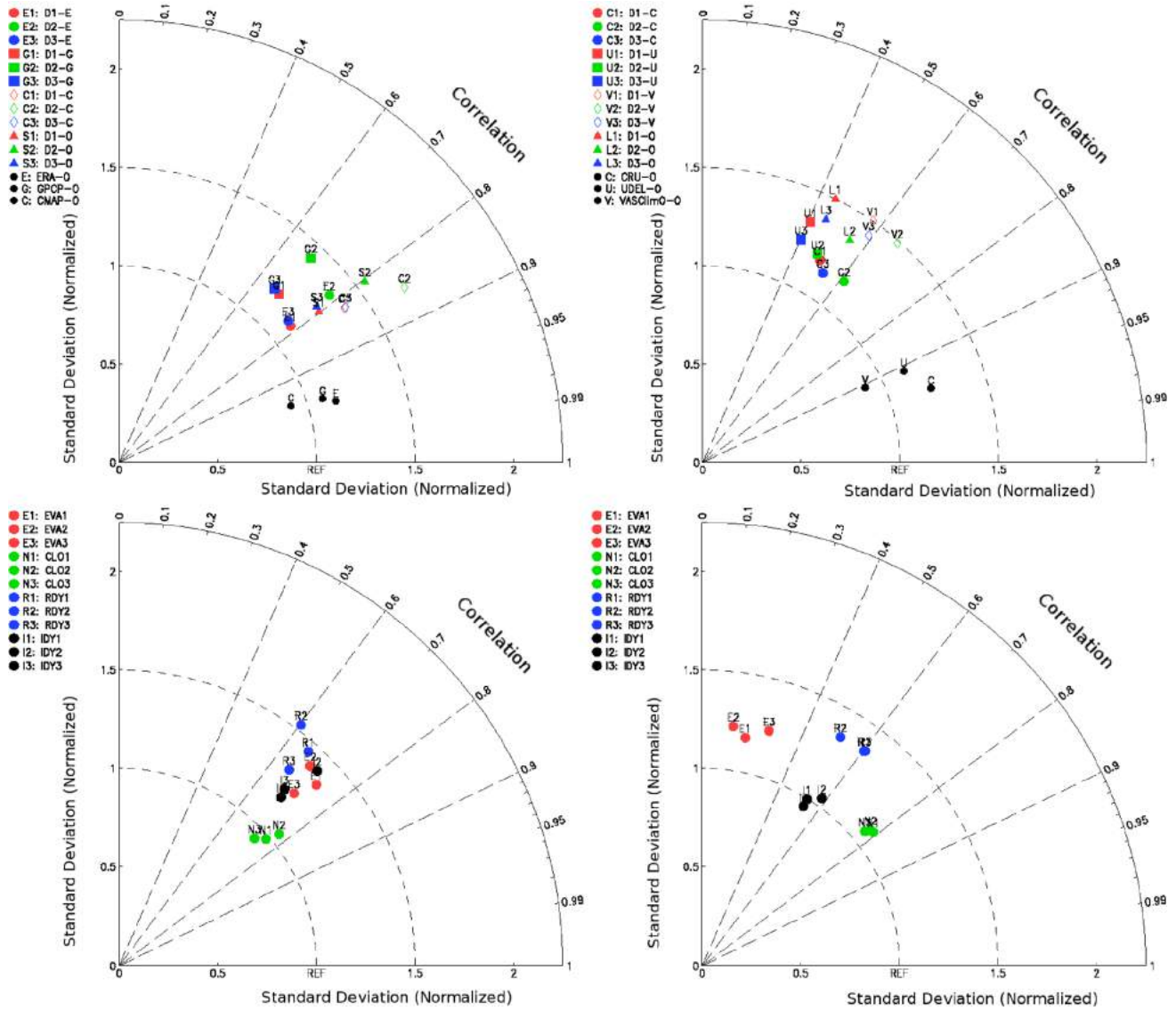

Fig. 7 EWS standardized deviations and spatial pattern correlations between the three domains and different references datasets for precipitation (*top row*) and cloud cover, moisture flux, rainfall frequency and intensity (*bottom row*). In the *top row* D1, D2 and D3 are indicated by *red*, *green* and *blue colors*, respectively; *colored circles*, *squares* and *diamonds* indicates whether the domains were compared with ERA, GPCP and CMAP, respectively, while the *triangles* indicate the comparison against the average of the three references; *black circles* represent the differences of each individual dataset and the simple average of the three. In the *bottom row* D1, D2 and D3 are indicated by 1 2 3, while the *colors red*, *green*, *blue* and *black* represent evaporation, cloud cover, rainfall frequency and rainfall intensity, respectively. In this case the reference dataset is the ERA reanalysis

August–October (late season) separated by a lower rainfall period (July–August) called the mid-summer drought/dry spell (Magaña et al. 1999; Gamble and Curtis 2008). Figure 8 shows the rainfall climatology for D1–3 over the three smaller areas defined in Fig. 1. The plots are averaged over all land + sea points and are compared to similarly derived climatologies from GPCP, ERA, CMAP (top row). The same is done for land grid points which are compared to climatologies from CRU, UDEL and VASclimO (bottom row).

From Fig. 8 the following are noted:

1. The model is able to reproduce the bimodal structure of the observed annual cycle.
2. For land + sea grid points the model tends to produce more precipitation than CMAP and GPCP products, except over the LCI subregion where the simulated rainfall shows a dry bias during the boreal summer.
3. The model mirrors the pattern of the ERA reanalysis with a wetter late season than early. However, the rela-

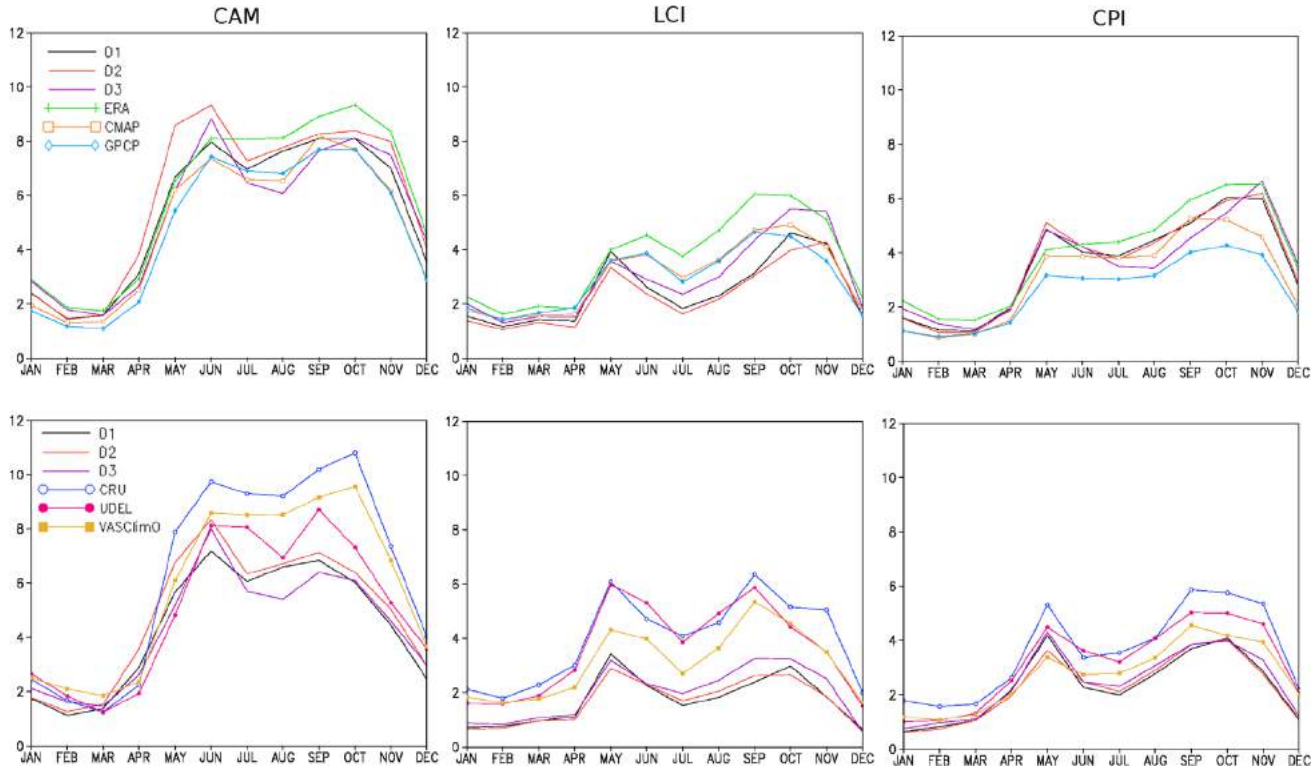

Fig. 8 Annual cycles of mean precipitation (mm/day) for observations and PRECIS simulations averaged over CVA, CAM, LCI and CPI for land-sea points (*top row*) and land points (*bottom row*)

tive minimum in July is more clearly represented by the model suggesting an added value of the RCM experiments. This is especially true for the CPI subregion where neither ERA reanalysis nor the other rainfall products reproduce the bimodal pattern. It is noted that if only land points are considered, all the observational datasets show the bimodal distribution, notwithstanding the differences between them, and the second peak in the modeled precipitation is no longer higher than the first.

4. The major differences between model and observed/reanalysis datasets occur over land areas and mostly during the wet season when less precipitation is simulated than observed. Over the LCI subregion the model exhibits a persistent dry bias throughout the entire year with largest bias occurring during the wet season as well.
5. Generally, there are no major differences between the domains in the modeled annual rainfall cycle. In fact, the discrepancies between the reference datasets are greater than the differences between model experiments for averages over all land + sea points. This is particularly noticeable during the wet months over all the sub-regions except for LCI.

Figure 9 shows the differences between the average of June and September rainfall and the average of July and August rainfall. These differences are used as a measure of the MSD signal (after Rauscher et al. 2008 and Diro et al. 2012) and facilitates an examination of how the model spatially reproduces the presence and strength of the MSD. Negative differences indicate the likely presence of the MSD, with magnitudes indicative of its severity.

From the rain gauge station based databases (Fig. 9, top row), the MSD is best defined over the western coast of Central America, the Yucatan Peninsula and Cuba but is absent in Southern Belize and on the Caribbean coast of Nicaragua and Costa Rica. Similar patterns are seen for the coarser resolution reanalysis products (Fig. 9, middle row) but with much less spatial details. Largest differences occur with CMAP which extends the MSD over almost all Central America but not over the Yucatan Peninsula. The domain experiments (Fig. 9, bottom row) broadly mirror the MSD spatial patterns, showing its occurrence over almost all the Pacific coast of Central America, the Yucatan and the western half of Cuba. The simulation, however, tends to extend the MSD too far east over Honduras and Nicaragua (particularly in D3) and also over southern Belize, where it is absent in the observations. The east–west gradient observed over Nicaragua is well captured by D1 and D2 (better in D1) but is not represented by D3. Over the Caribbean Islands the simulated MSD

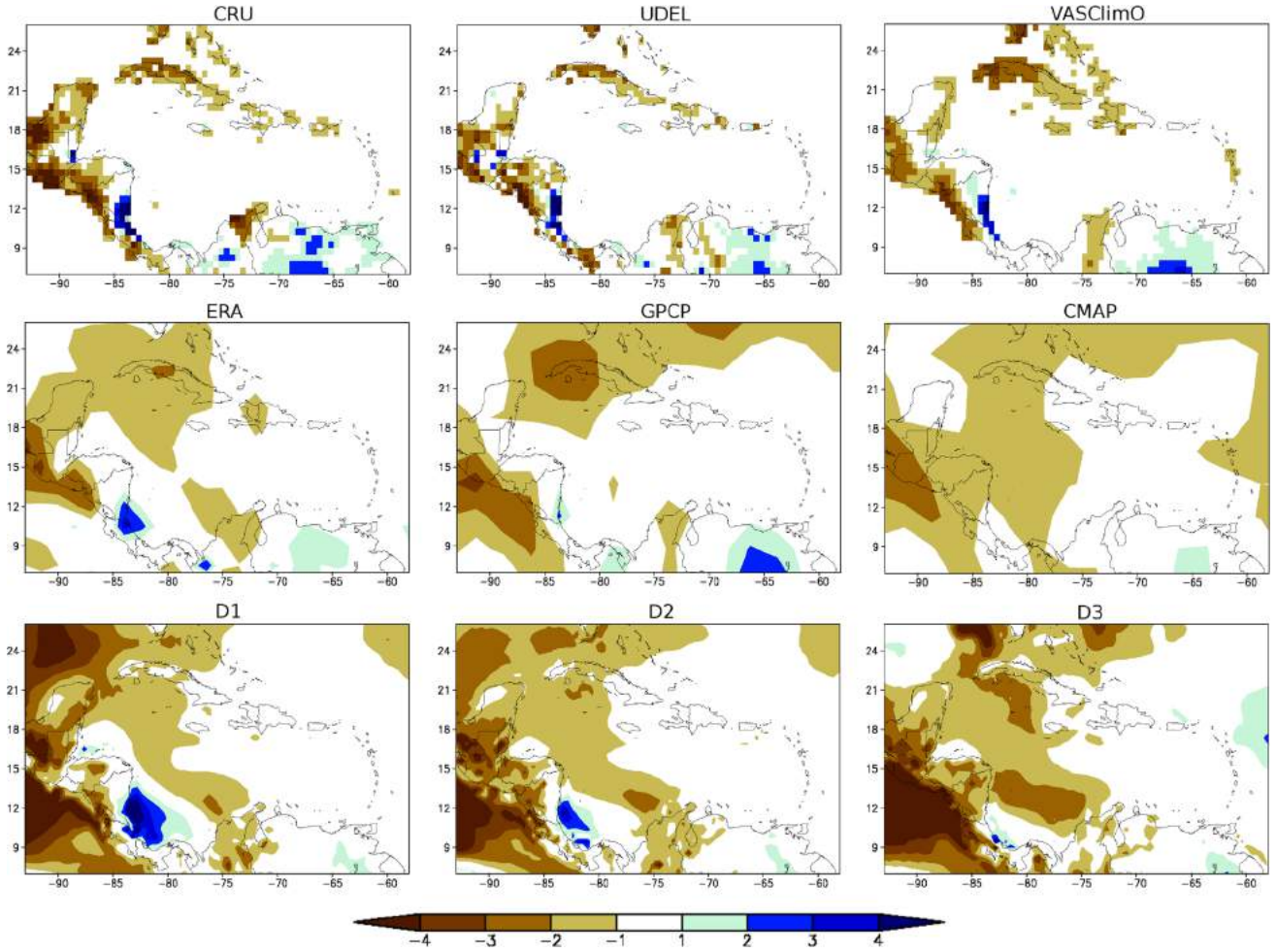

Fig. 9 MSD precipitation indicator 1991–1999 for CRU, UDEL and VASclimO observed rainfall over land, ERA, GPCP and CMAP reanalysis and D1–3 simulations. *Brown regions* indicate the presence of MSD

signal is weaker than observed and is largely confined to parts of western Cuba.

The MSD is associated with an intensification and westward shift of the NASH and an increase in the low-level easterly wind strength over the Caribbean Sea and the Gulf of Mexico (Hastenrath 1966; Magaña et al. 1999; Giannini et al. 2000). The RCM results are examined for their ability to reproduce these changes. Figure 10 (top row) shows changes in sea level pressure (SLP) and low-level wind with respect to prior month values for ERA reanalysis for May through August. A decrease in SLP over the Gulf of Mexico and the Caribbean at the start of the EWS in May is followed by an increase in June throughout the eastern Caribbean. This June increase in the NASH's influence is accompanied by an anticyclonic circulation anomaly pattern i.e. easterly anomalies over the Caribbean Sea and southerly anomaly over the Yucatan, Cuba and Hispaniola. In July, the strong influence of the NASH is evident in the increase in SLP over the entire CVA region, which is accompanied by a cyclonic (anticyclonic) circulation anomaly over the eastern Caribbean (western half of the CVA). There are also northerly anomalies over the Gulf of Mexico and easterly anomalies over the Caribbean Sea.

The SLP and low-level winds obtained from ERA are closely mirrored by the simulations (Fig. 10, rows 2–4) with minor differences. The negative change in SLP from April to May is greater in the PRECIS simulations, being more intense for D1. Positive SLP changes in June are shifted further west over Cuba, the western Caribbean Sea and Central America, except in D3, where negative changes persist over areas of Central America. D1 and D3 also show negative SLP values over the top-left corner of the CVA coincident with stronger southern wind anomalies. The further increase in SLP in July is well simulated for all domains, though in D3 the eastern area of weaker positive change is extended westward over La Hispaniola. In addition an area of negative change not seen in the reanalysis is simulated near the eastern border of the CVA in D3,

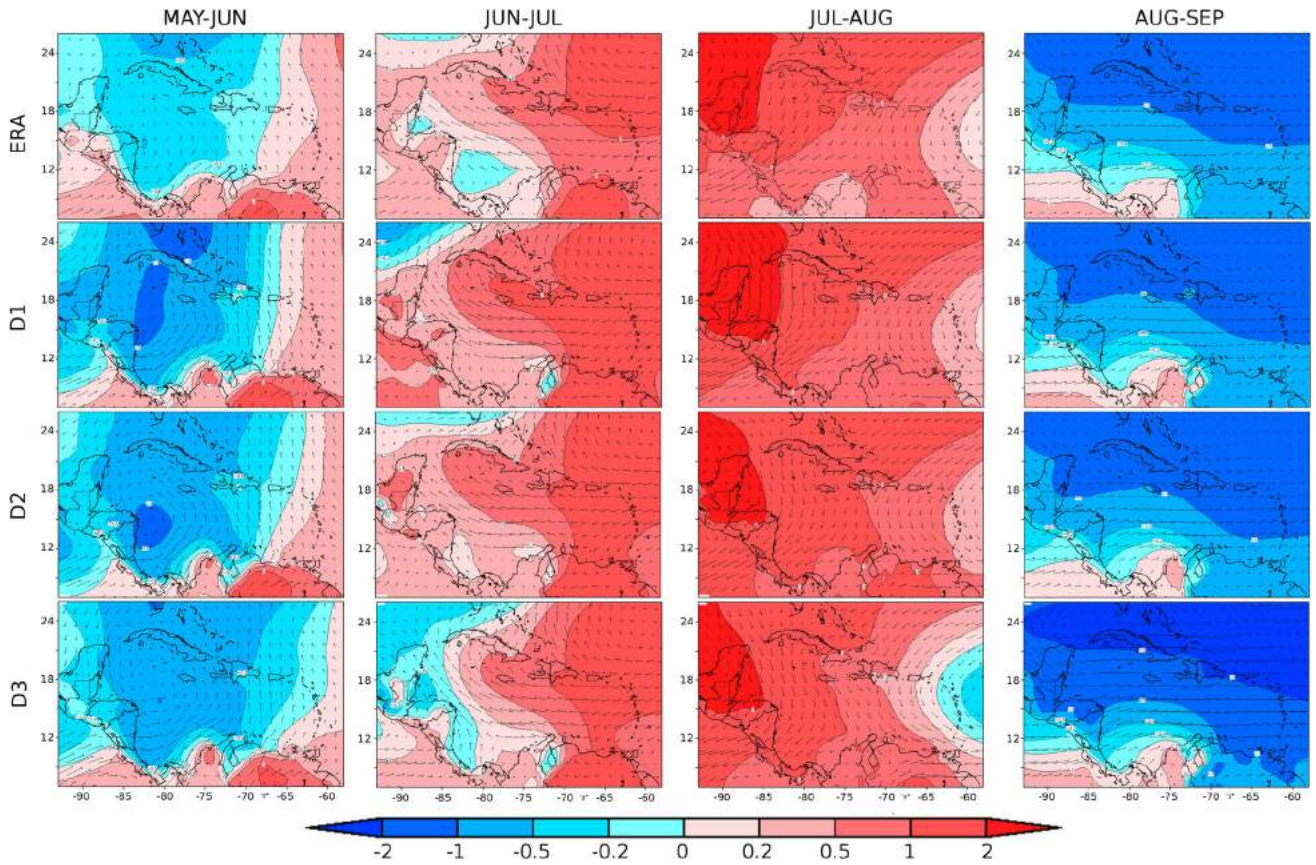

Fig. 10 Month-to-month differences in sea level pressure (hPa) and 925 hPa wind vectors for ERA reanalysis, D1–3 from *top* to *bottom rows*, respectively. Positive (negative) SLP are in *red* (*blue*)

strengthening the low-level cyclonic circulation anomaly in this region. The simulations reproduce the SLP reduction in August, but for D3 the negative anomalies are shifted southward, resulting in a stronger meridional SLP gradient over the southwestern Caribbean Sea accompanied by a slightly stronger westerly circulation anomaly. In comparison to D1 and D2, the stronger easterly flow in D3 could account for the simulated rainfall reduction in August over CAM for this domain (Fig. 8, land grid points) and for the extension of the MSD signal over almost all Central America (see again Fig. 9).

The Taylor diagrams shown in Fig. 11 do not suggest a strong impact of domain size on either the Caribbean rainfall annual cycle or the regional atmospheric circulation associated with the MSD and the NASH influence. With respect to the annual cycle (Fig. 11, left panel), the RCMs tend to have smaller amplitudes than observed but are accurately phased with correlations greater than 0.9 over land areas (greater than 0.8 over land + sea points, not shown). There are no clear differences between the performance of the different configurations and the worst simulations seemingly occur for the LCI subregion. The spread amongst the observed datasets for the different subregions is also evident. With respect to the simulated atmospheric circulation features related to the MSD and the NASH influence (i. e. month-to-month low-level wind and SLP as well as MSD low-level wind) (Fig. 11, right panel) D2 appears as a marginally more skillful experiment with correlation greater that 0.9 and amplitudes closer to ERA reanalysis. The other two configurations also have high correlations (greater that 0.8) but with slightly higher amplitudes and RMS differences.

3.3 The Caribbean low-level jet and seasonal low-level circulation

The CLLJ manifests as a strong increase in the trades up to 700 hPa over a region delimited by 70°W–80°W, 12°N–15°N, with maximum horizontal wind speeds of up to 16 m/s at 925 hPa (Amador 1998; Amador and Magaña 1999; Amador et al. 2000). Several studies associate the CLLJ with (1) the formation of the MSD over Central America (Magaña et al. 1999), (2) intense rainfall over the Central America Atlantic coast (Amador and Magaña 1999), (3) a minimum of tropical cyclones and a maximum of SLP in the Caribbean region (Wang 2007) and (4)

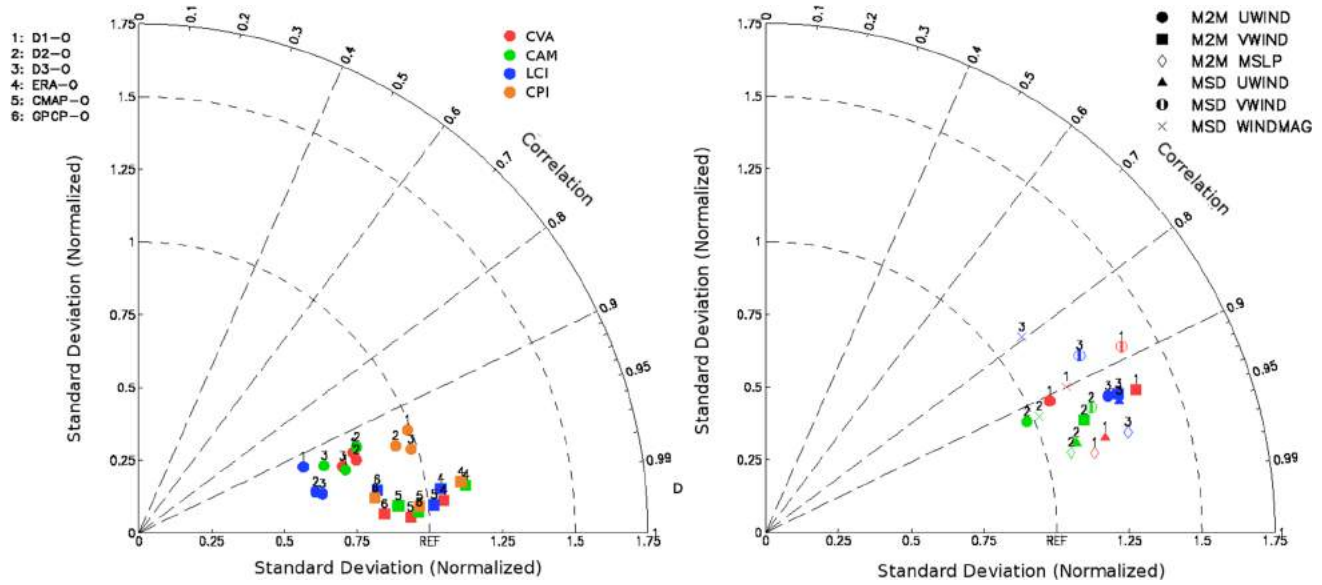

Fig. 11 Taylor diagrams for the land-sea grid points rainfall annual cycle in the CVA and the subregions (*left*) and month-to-month variations of atmospheric circulation as well as the low-level MSD circulation pattern (*right*). In the *left panel* the numbers 1, 2, 3 indicate D1, D2, D3 and 4, 5, 6 represents to ERA, CMAO and GPCP, respectively, while the *red*, *green*, *blue* and *orange color* indicate the CVA and the CAM, LCI and CPI subregions. In the *right panel* D1, D2 and D3 are indicate by *red*, *green* and *blue colors*, respectively; *circles*, *squares*, *triangles*, multiplication sign, and *circle with vertical bar*, represent month-to-month zonal wind, meridional wind and SLP as well as zonal wind, meridional wind and wind magnitude, respectively

rainfall anomalies over the Caribbean (Wang 2007; Whyte et al. 2008). The CLLJ also appears as the first mode of the zonal wind in July (Whyte et al. 2008). Whyte et al. (2008) locates the east–west jet axis at approximately 15°N and limits its vertical and meridional extent to the trade wind inversion and to the Andes to the south, respectively. The RCM's ability to simulate the CLLJ's is examined as well as other features of the low-level regional circulation. Figure 12 presents the annual cycle of the 925 hPa zonal wind averaged over 12.5°N–17.5°N, 80°W–70°W, which is the region normally used to define CLLJ index (Wang 2007; Whyte et al. 2008). D1 and D2 simulations produce a peak of maximum wind speed in July similar to that seen in ERA but overestimate the zonal wind speed early in the year. In contrast, D3 underestimates the speed during the summer months and produces a peak in June instead of July. It should be noted that there are substantial differences in the portrayal of the CLLJ annual cycle in ERA and NARR. NARR has zonal wind speed values for the CLLJ index which are lower than ERA and than that found in the peer-reviewed literature (e.g. Amador 1998; Wang 2007; Whyte et al. 2008). Notwithstanding that NARR is a higher resolution reanalysis, it does not accurately capture the CLLJ intensity even though it reasonably represents the shape of the annual cycle.

Figure 13 shows that the spatial patterns of zonal and total wind at 925 hPa in July are well-simulated by the RCM, especially for D1 and D2 configurations. Features

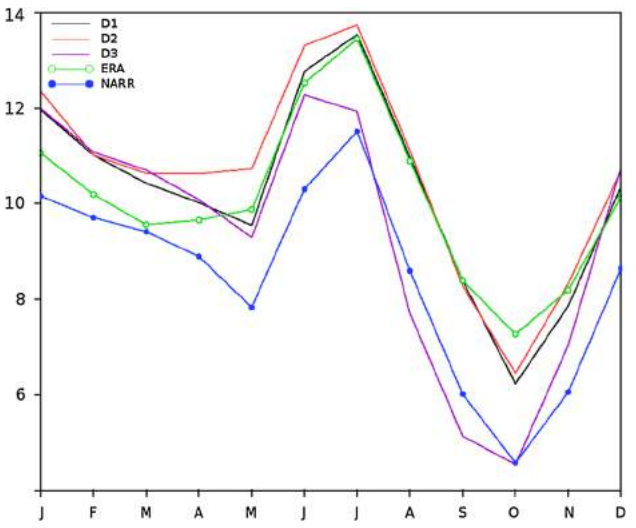

Fig. 12 Annual cycle of zonal wind at 925 hPa (multiplying by −1) averaged over the CLLJ region (12.5°N–17.5°N, 80°W–70°W) for ERA and NARR reanalysis and D1–3 model experiments

such as the east–west band of strong easterly zonal wind located along 13°N, and the two exit regions of strengthened easterlies in the southwestern Caribbean and in the north (close to 18°N) are well-reproduced, though they are weaker (stronger) than observations in D1 (D2). Very strong in the northern exit region suggest a possible strengthening of the simulated Great Plain Low Level

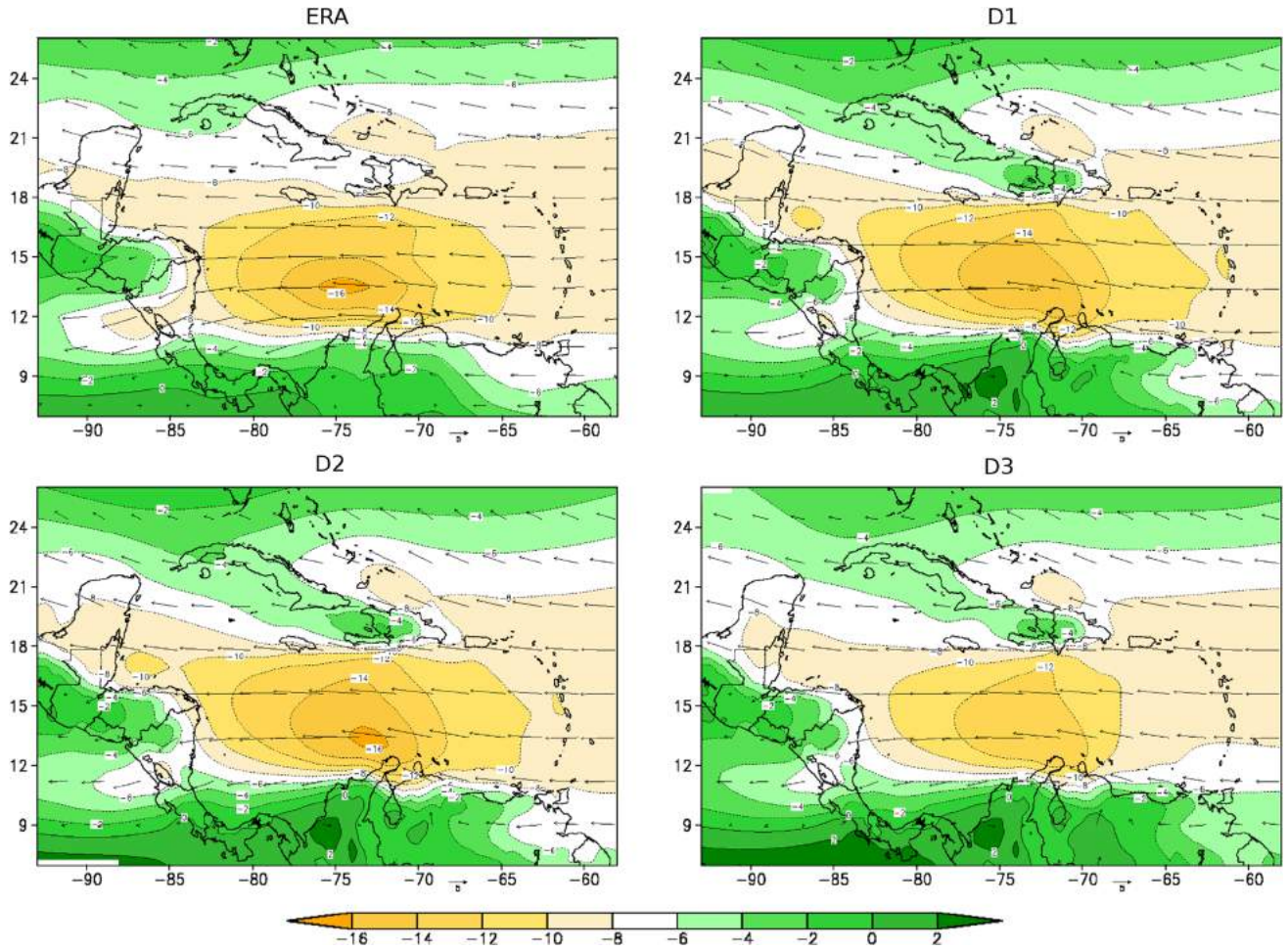

Fig. 13 1991–1999 July mean zonal wind (*shaded*) and total wind (*vectors*) for ERA reanalysis and D1–3 experiments

Jet which is connected to this branch of the CLLJ. It is noted, however, that the area of maximum wind (~16 m/s) appears clearly defined in D2 only and the region of winds higher than 14 m/s is extended slightly more to the north in D1 and D2. For D3, maximum wind values associated with the CLLJ do not reach 14 m/s. Differences in the modeled low-level wind fields compared to ERA also occur over La Hispaniola and to a lesser extent west of Puerto Rico and Jamaica and over the eastern half of Cuba where the zonal wind strength is lower. These differences suggest the effect of both mountain regions and land-sea contrast on the easterly flow which is not seen in the lower resolution ERA dataset but which are evident in (for example) higher resolution reanalysis such as NARR (not shown).

Finally, variations in the vertical structure of the atmosphere with latitude are generally very well-reproduced by each of the RCM simulations (Fig. 14). The simulations capture the dominant easterly flow during boreal summer, the stronger low-level winds between 12 and 18°N related with the CLLJ, and the position of the trade wind inversion. However, for D3 there is a reduced vertical gradient of the zonal wind component as a result of weaker easterly low-level flow. In general, the simulated vertical structure of the circulation suggests enhanced vertical wind shear, where the shear is calculated as the difference between 200 and 850 hPa of the magnitude of horizontal wind. The spatial distribution of vertical wind shear anomalies (not shown) is similar for D1 and D2 except that highest positive shear anomalies are placed over the Pacific in D1 versus over the central and western Caribbean Sea in D2. The D3 configuration produces a very different vertical shear anomaly pattern with positive differences confined to the western half of the CVA and negative differences extending into the southwestern Caribbean. The simulated shear patterns likely further contribute to the systematic negative rainfall bias of all simulations by preventing the organization of deep convection, limiting the occurrence of heavy rainfall events and reducing the formation of tropical cyclones (Inoue et al. 2002; Wang 2007).

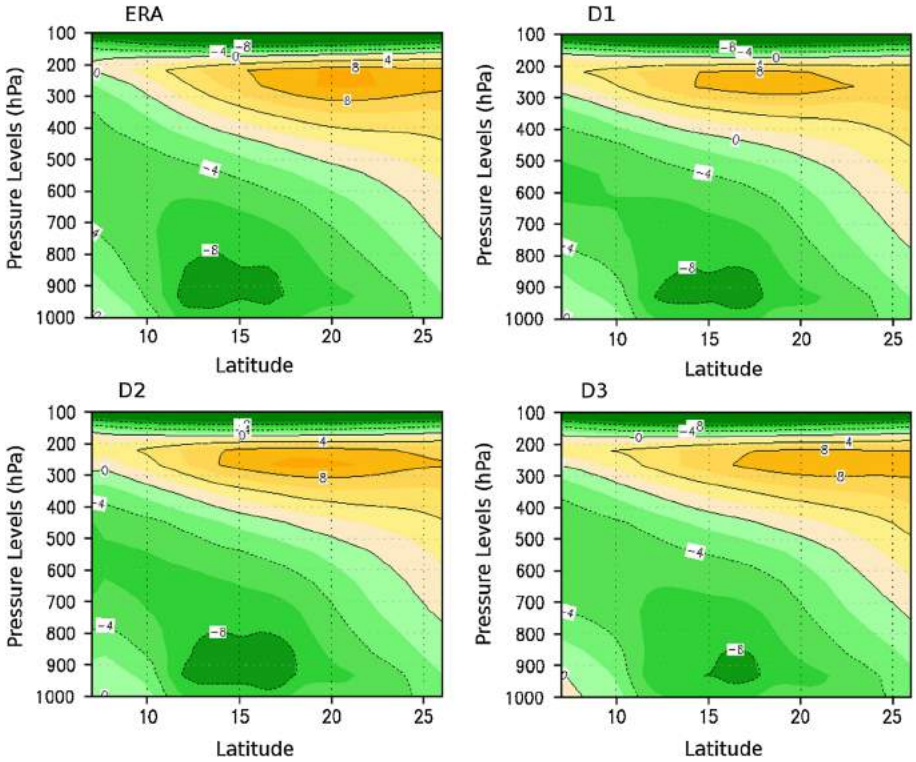

Fig. 14 1991–1999 mean zonal wind (easterlies in *green* and westerlies in *yellow*) zonally averaged over the CVA for MJJ of ERA and D1–3 domains (*from top to bottom*)

4 Summary and conclusions

In this paper the impact of three different domain sizes on simulated regional patterns of precipitation and atmospheric circulation features of the Caribbean was assessed using the PRECIS RCM. The overall skill of PRECIS in reproducing key climate regional characteristics was also evaluated for the early (MJJ) and late (ASO) wet seasons.

With respect to model performance we note the following:

1. *The skill of the model in reproducing large-scale processes*: The three RCM configurations simulate reasonably well the synoptic scale climatological patterns of precipitation across the Caribbean during the wet season, including the maximum off the Caribbean coastline of Panama, and the dry belt over the southern Dutch Caribbean Islands. Relevant features of the rainfall annual cycle over the defined subregions are also well reproduced by PRECIS for all domains. These include the distinction between the EWS and LWS and the relative rainfall reduction in July–August associated with the MSD. The model biases are similar to those found by Campbell et al. (2010). The difference between the latter study and this one is the driving data, suggesting that the simulated biases are are mainly due to the internal characteristics of PRECIS RCM over Caribbean i.e. they are independent of the driving information.
2. *The importance of land processes*: The model underestimates precipitation over most of the domain but particularly over land areas. The systematic overland dry bias of PRECIS appears to be related to an underestimation of the large-scale rainfall but also to a weaker over-land hydrological cycle associated with less soil moisture being available for evaporation. The latter would yield less surface latent heat flux to the atmosphere and reduce the evaporative cooling of the atmosphere. In support of this, it is noted that the model (irrespective of configuration) exhibits a positive bias in mean tropospheric temperature of ~1.0 °C at 1,000 hPa and up to 0.6 °C at levels below 300 hPa (not shown). This would also help explain the warm bias in model simulations noted by Campbell et al. (2010).
3. *Resolution and small islands climates*: The added value of the RCM over (for example) ERA is seen in its better representation of the land-sea mask and orography and the impact this seemingly has on the simulated climate e.g. the apparent impact on the easterly flow (see again discussion of Fig. 13). It is noted, however, that the simulations produced a rainfall shadow leeward of the islands which we also associate with the RCM's sensitivity to land surface and topography configuration. The phenomenon is also seen in high spatial resolution datasets such as TRMM but to a lesser extent. Although the effect appears over the sea adjacent to the landmasses, it may influence simulated rain-

fall amounts over the nearest land grid points, and for this reason bears further investigation, especially with respect to improving the PRECIS model's performance over regions with small islands.

With respect to the choice of domain we make the following observations:

- Discernible discrepancies between the PRECIS configurations with respect to simulated rainfall are not seemingly significant when both land and sea grid points are considered. When land-only points are analyzed the overall model ability decreases and D2 appears as the most skillful simulation (see again Fig. 7), but the differences with the other domains are not substantial.
- The analysis of simulated cloud cover, evaporation, and rainfall frequency and intensity also suggests a similarity between the domains, making it difficult to identify a better domain configuration.
- The atmospheric circulation patterns associated with the MSD, including the influence of the NASH during the year, are reasonably reproduced by the three configurations. In this instance, D2 appears to be the best of all three simulations (see again discussion related to Fig. 11).
- The CLLJ is well reproduced by PRECIS over the D1 and D2 configurations. For D2, the simulated annual cycle is slightly stronger than observed, especially in July. There is also a stronger vertical gradient of the wind field, and a stronger wind shear over the Caribbean Sea than seen in the ERA dataset (also seen in D1). The stronger vertical wind shear patterns likely contribute to the systematic negative rainfall bias in the simulations, but may not be the main determinant since the dry bias is also observed in D3 where the vertical shear is in fact weaker. The model simulates simulates a weaker easterly low-level flow for D3.

In general, the three domain configurations show more similarities than differences in the simulated results especially for D1 and D2. A reduction in domain size does not significantly impact the atmospheric circulation patterns, especially at the low level. More specifically, extending the domain further to east, as in D3, does not seem to yield substantially significant improvements, as some features of the regional circulation are less well represented in comparison to D1 and D2.

We conclude, then, that even though both D1 and D2 present as good candidates for simulating the climate of the region and producing future climate projections, D2 may represent an optimal choice given the computational and other resource constraints of Caribbean institutions. This may have implications for future regional projects targeting the use of regional models including those geared toward participation in global efforts like CORDEX.

Finally, though the PRECIS RCM has been extensively used and evaluated over European, Asian and African domains, this study highlights the importance of also evaluating it over a geographically different region like the Caribbean where small land areas are surrounded by large bodies of water. As has been shown there is some value added by the inclusion of the land mass and topography of the small islands in the RCM.

Acknowledgments This work was conducted as part of a collaborative effort between Instituto de Meteorologia (Cuba), the Climate Studies Group Mona (CSGM) of the University of the West Indies (Jamaica), the Cave Hill campus of the University of the West Indies (Barbados) and the Antom de Kom University (Suriname) under the Caribbean Modelling Initiative. The collaboration was funded by the Caribbean Community Climate Change Centre (Belize) and the Climate Change Adaptation and Mitigation Research Program of the Ministry of Science, Technology and Environment (CITMA) of Cuba. INSMET's participation was partially funded by the Climate and Development Knowledge Network (CDKN) project CARIWIG and by the 'The Future of Climate Extremes in the Caribbean' (XCUBE). XCUBE is a joint project between Norway and Cuba funded by the Direktoratet for samfunnssikkerhet og beredskap (DSB) on an assignment for the Norwegian Ministry of Foreign Affairs. The CSGM participation was partially funded by the GoLoCarSce project under the ACP-EU Science and Technology Programme. Special thanks to Dr. Richard G. Jones for instructive comments. Thanks also to the Hadley Centre (UK) for PRECIS model support. Thanks to the anonymous reviewers whose helpful comments allowed us to improve the paper.

References

Adler R, Huffman G, Chang A, Ferraro R et al (2003) The Version 2 global precipitation climatology project (GPCP) monthly precipitation analysis (1979—present). J Hydrometeor 4:1147–1167

Alfonso AP, Naranjo LR (1996) The 13 March 1993 severe squall line over Western Cuba. Weather Forecast 11:89–102

Amador JA (1998) A climatic feature of the tropical Americas: the trade wind easterly jet. Top Meteor Oceanogr 5:1–13

Amador JA, Magaña VO (1999) Dynamics of the low level jet over the Caribbean sea. Preprints, 23rd conference on hurricanes and tropical meteorology. American Meteorological Society, Dallas, TX, pp 868–869

Amador JA, Magaña VO, Pérez JB (2000) The low level jet and convective activity in the Caribbean. Preprints 24th conference in hurricanes and tropical meteorology. American Meteorological Society, Fort Lauderdale, FL, pp 114–115

Beck C, Grieser J, Rudolf B (2005) A new monthly precipitation climatology for the global land areas for the period 1951 to 2000. DWD, Klimastatusbericht 2004:181–190

Bhaskaran B, Jones RG, Murphy JM, Noguer M (1996) Simulations of the Indian summer monsoon using a nested regional climate model: domain size experiments. Clim Dyn 12:573–587

Campbell JD, Taylor MA, Stephenson TS, Watson RA, Whyte FS (2010) Future climate of the Caribbean from a regional climate model. Int J Climatol. doi:10.1002/joc.2200

Centella A, Bezanilla A, Leslie K (2008) A study of the uncertainty in future Caribbean climate using the PRECIS regional climate model. Technical Report. Community Caribbean Climate Change Center, Belmopan, 16 pp

Chen AA, Taylor MA (2002) Investigating the link between early season Caribbean rainfall and the El Niño +1 year. Int J Climatol 22:87–106

Chen AA, Roy A, McTavish J, Taylor MA, Marx L (1997) Using SST anomalies to predict flood and drought conditions for the Caribbean. COLA Report 49

Christensen J, Machenhauer HB, Jones RG, Shär C, Ruti PM, Castro M, Visconti G (1997) Validation of present-day climate simulations over Europe: LAM simulations with observed boundary conditions. Clim Dyn 13:489–506

Colin J, Déqué M, Radu R, Somot S (2010) Sensitivity study of heavy precipitation in limited area model climate simulations: influence of the size of the domain and the use of the spectral nudging technique. Tellus A 62:591–604. doi:10.1111/j.1600-0870.2010.00467.x

Dee DP, Uppala SM, Simmons AJ, Berrisford P, Poli P, Kobayashi S, Andrae U, Balmaseda MA, Balsamo G, Bauer P, Bechtold P, Beljaars ACM, van de Berg L, Bidlot J, Bormann N, Delsol C, Dragani R, Fuentes M, Geer AJ, Haimberger L, Healy SB, Hersbach H, Hólm EV, Isaksen L, Kållberg P, Köhler M, Matricardi M, McNally AP, Monge-Sanz BM, Morcrette JJ, Park BK, Peubey C, de Rosnay P, Tavolato C, Thépaut JN, Vitart F (2011) The ERA-Interim reanalysis: configuration and performance of the data assimilation system. QJR Meteorol Soc 137:553–597. doi:10.1002/qj.828

Denis B, Laprise R, Caya D, Cote J (2002) Downscaling ability of one-way nested regional climate models: the big-brother experiment. Clim Dyn 18:627–646

Diro GT, Rausher SA, Giorgi F, Tompkins AM (2012) Sensitivity of seasonal climate and diurnal precipitation over Central America to land and sea surface schemes in RegCM4. Clim Res 52:31–48

Gamble DW, Curtis S (2008) Caribbean precipitation: review, model and prospect. Prog Phys Geography 32(3):265–276

Giannini A, Kushnir Y, Cane MA (2000) Inter-anual variability of Caribbean rainfall, ENSO, and the Atlantic Ocean. J Clim 13:297–311

Giorgi F, Mearns L (1999) Regional climate modeling revisited. J Geophys Res 104:6335–6352

Granger OE (1985) Caribbean climates. Prog Phys Geography 9:16–43

Hastenrath S (1966) On general circulation and energy budget in the area of the Central American seas. J Atmos Sci 23:694–711

Hastenrath S (1967) Rainfall distribution and regimes in Central America. Arch Meteor Geophys Bioclimatol Ser B 15:201–241

Huffman GJ, Adler RF, Morrissey MM, Bolvin DT, Curtis S, Joyce R, McGavock B, Susskind J (2001) Global precipitation at one-degree daily resolution from multisatellite observations. J Hydrometeor 2:36–50

Huffman GJ, Adler RF, Bolvin DT, Gu G, Nelkin EJ, Bowman KP, Stocker EF, Wolff DB (2007) The TRMM multi-satellite precipitation analysis: quasi-global, multi-year, combined-sensor precipitation estimates at fine scale. J Hydrometeor 8:33–55

Huntingford C, Jones RG, Prudhomme C, Lamb R, Gash JH, Jones A (2003) Regional climate-model predictions of extreme rainfall for a changing climate. QJR Meteorol Soc 129:1607–1621

Inoue M, Handoh IC, Bigg GR (2002) Bimodal distribution of tropical cyclogenesis in the Caribbean: characteristics and environmental factors. J Clim 15:2897–2905

IPCC (2007) Climate change (2007): the physical science basis. Contribution of working group I (WGI) to the fourth assessment report (AR4) of the Intergovernmental Panel on Climate Change (IPCC) [Solomon S, Qin D, Manning M, Chen Z, Marquis M, Averyt KB, Tignor M, Miller HL (eds)]. Cambridge University Press, Cambridge

Jacob D, Podzun R (1997) Sensitivity studies with the regional climate model REMO. Meteorol Atmos Phys 63:119–129

Jones RG, Murphy JM, Noguer M (1995) Simulation of climate change over Eure using a nested regional climate model. Part I: assessment of control climate, including sensitivity to location of lateral boundaries. QJR Meteorol Soc 121:1413–1449

Jones RG, Murphy JM, Noguer M, Keen AB (1997) Simulation of climate change over Europe using a nested regional-climate model. Part II: comparison of driving and regional model responses to a doubling of carbon dioxide. QJR Meteorol Soc 123:265–292

Jones RG, Noguer M, Hassel D, Hudson D, Wilson S, Jenkins G, Mitchell J (2004) Generating high resolution climate change scenarios using HadRM3P. Met Office Hadley Centre Report, p 40

Kalnay E, Kanamitsu M, Kistler R, Collins W, Deaven D, Gandin L, Iredell M, Saha S, White G, Woollen J, Zhu Y, Leetmaa A, Reynolds R, Chelliah M, Ebisuzaki M, Higgins M, Janowiak J, Mo KC, Ropelewski C, Wang J, Jenne R, Joseph D (1996) The NCEP/NCAR 40-year reanalysis project. Bull Am Meteorol Soc 77(3):437–471

Kanamitsu M, Ebisuaki W, Woollen J, Yang SK, Hnilo JJ, Fiorino M, Potter GL (2002) NCEP/DOE AMIP-II reanalysis (R-2). Bull Am Meteorol Soc 83:1631–1643

Karmalkar AV, Bradley RS, Diaz HF (2008) Climate change scenario for Costa Rican montane forests. Geophys Res Lett 35:L11702

Karmalkar AV, Taylor MA, Campbell J, Stephenson T, New M, Centella A, Bezanilla A, Charlery J (2012) A review of observed and projected changes in climate for the islands in the Caribbean. Atmos 26:283–309

Magaña V, Amador JA, Medina S (1999) The midsummer drought over Mexico and Central America. J Clim 12:1577–1588

Martinez-Castro D, Porfirio da Rocha R, Bezanilla-Morlot A, Alvarez-Escudero L, Reyes-Fernandez JP, Silva-Vidal Y, Arritt RW (2006) Sensitivity studies of the RegCM3 simulation of summer precipitation, temperature and local wind field in the Caribbean region. Theoret Appl Climatol 86:5–22

Matsuura K, Willmott (2007) Terrestrial precipitation: 1900–2006 gridded monthly time series (version 1.01). http://climate.geog.udel.edu/~climate/html_pages/Global_ts_2007/README.global.p_ts_2007html

Mesinger F et al (2006) North American regional reanalysis. Bull Am Meteorol Soc 87:343–360

Mitchell TD, Jones PD (2005) An improved method of constructing a database of monthly climate observations and associated high-resolution grids. Int J Climatol 25:693–712

Rauscher SA, Giorgi F, Diffenbaugh NS, Seth A (2008) Extension and Intensification of the Meso-American mid-summer drought in the twenty-first century. Clim Dyn 31:551–571

Rayner NA, Parker DE, Horton EB, Folland CK, Alexander LV, Rowell DP, Kent EC, Kaplan A (2003) Global analyses of sea surface temperature, sea ice, and night marine air temperature since the late nineteenth century. J Geophys Res 108(D14):4407. doi:10.1029/2002JD002670

Riehl H (1979) Climate and weather in the tropics. Academic Press, London, p 595

Rossow WB, Schiffer RA (1991) ISCCP cloud data products. Bull Am Meteorol Soc 72:2–20

Seneviratne SI, Nicholls N, Easterling D, Goodess CM, Kanae S, Kossin J, Luo Y, Marengo J, McInnes K, Rahimi M, Reichstein M, Sorteberg A, Vera C, Zhang X (2012) Changes in climate extremes and their impacts on the natural physical environment. In: Field CB, Barros V, Stocker TF, Qin D, Dokken DJ, Ebi KL, Mastrandrea MD, Mach KJ, Plattner G-K, Allen SK, Tignor M, Midgley PM (eds) Managing the risks of extreme events and disasters to advance climate change adaptation. A special report of working groups I and II of the Intergovernmental Panel on Climate Change, pp 109–230

Seth A, Giorgi F (1998) The effects of domain choice on summer precipitation simulation and sensitivity in a regional climate model. J Clim 11:2698–2712

Simmons AJ, Burridge DM (1981) An energy and angular-momentum conserving vertical finite difference scheme and hybrid vertical coordinates. Mon Weather Rev 109:758–766

Simmons A, Dee D, Uppala S, Kobayashi S (2007) Era-interim: new ECMWF reanalysis products from 1989 onwards. In: ECMWF Newsl, 110. ECMWF, pp 29–35

Stephenson TS, Chen AA, Taylor MA (2007) Toward the development of prediction models for the primary Caribbean dry season. Theoret Appl Climatol 92:87–101

Taylor KE (2001) Summarizing multiple aspects of model performance in a single diagram. J Geophys Res 106:7183–7192

Taylor MA, Enfield DB, Chen AA (2002) The influence of the tropical Atlantic vs. the tropical Pacific on Caribbean rainfall. J Geophys Res 107(C9):3127. doi:10.1029/2001JC001097

Taylor MA, Stephenson TS, Owino A, Chen AA, Campbell JD (2011) Tropical gradient influences on Caribbean rainfall. J Geophys Res. doi:10.1029/2010JD015580

Taylor MA, Centella A, Charlery J, Bezanilla A, Campbell JD, Borrajero I, Stephenson TS, Nurmohamed R (2013) The precis Caribbean story: lessons and legacies. Bull Am Meteorol Soc 94:1065–1073

Tourigny E, Jones CG (2009) An analysis of regional climate model performance over the tropical Americas. I. Simulating seasonal variability of precipitation associated with ENSO forcing. Tellus Ser A 61:323–342

Wang C (2007) Variability of the Caribbean low-level jet and its relations to climate. Clim Dyn 29:411–422

Wang C, Lee SK (2007) Atlantic warm pool, Caribbean low-level jet and their potential impact on Atlantic hurricanes. Geophys Res Lett 34:L02703

Whyte FS, Taylor MA, Stephenson TS, Campbell JD (2008) Features of the Caribbean low level jet. Int J Climatol 28:119–128

Xie P, Arkin PA (1997) Global precipitation: A 17-year monthly analysis based on gauge observations, satellite estimates, and numerical model outputs. Bull Am Meteorol Soc 78(11):2539–2558